The thermal analysis of the hard X-ray telescope (HXT) and the investigation of the deformation of the mirror foil due to temperature change

Keitaro Ito*[a], Keiji Ogi*[a], Hisamitsu Awaki*[a], Tatsuro Kosaka*[b], Yasufumi Yamamoto*[a]
[a]Ehime University, [b]Kochi University of Technology

ABSTRACT

The thin film technology called “depth-graded multi-layer” is used to manufacture reflector foils, which are inserted in a hard X-ray telescope. The foil is constructed of an aluminum substrate, epoxy adhesion layer and a platinum/carbon multi-layered reflecting surface. When the temperature of the foil changes from the temperature at which the foil was produced; thermal deformation is induced due to difference of linear coefficient of expansion of its constituents. The deformation causes performance of X-ray image formation to deteriorate. Therefore, it is absolutely imperative to estimate the amount of deformation quantitatively and to establish a method of temperature control for the foil under the thermal environment on orbit. We used the hard X-ray telescope, which is part of the currently-projected the ASTRO-H X-ray satellite, as an example for investigation. The effective method of the HXT thermal control was examined with the thermal analytical software, ”Thermal Desktop”. The deformation of the foil when the temperature was changed by 1 degree C was predicted by a finite element analysis (FEA). The experiment on the foil was also performed and the test results were compared with the FEA. The thermal desktop analysis shows that the overall foil temperature in orbit can be close to the temperature at which the foils were produced (~22degree C) by the newly developed thermal control method. The FEM analysis shows that the prediction of the foil deformation due to a temperature change of 1 degree C is about 8 μm. We will measure the influence of the deformation on performance of the X-ray image formation in the future.

Introduction

Our group is developing a hard X-ray telescope (HXT) as one of the onboard instruments for Astro-H.
Since thin films for reflecting X-rays was adhesively bonded inside of the foils, thermal deformation is induced due to mismatch of thermal expansion coefficients of constituent materials when the temperature of the foils is changed from that at manufacturing (295.15 K). Such thermal deformation may cause degradation of quality of the X-rays image. The amount of thermal deformation in the generating line direction must be less than 10 mm. Hence, we have to establish the strategy for controlling the temperature of the foils, in addition to determining the allowable temperature range, by predicting thermal deformation of the foils quantitatively.

Thermal radiation analysis

Outline

The target temperature of the HXT on orbit is ranging from 293.15 K to 297.15 K. In order to analyze the temperature distribution of the housing and foils, a thermo-fluid analysis software "Thermal Desktop" (Ver. 2005) was employed.

The Hot and Cold Cases, in which the temperature of the satellite becomes the maximum and minimum, respectively, are considered in the following analysis.

Analysis 1	The temperature distribution of the foils when the temperature of the housing is kept at 295.15 K	Investigate whether the temperature of the foils is kept within the allowable temperature range when the temperature of the housing is maintained at 295.15 K by the heater equipped to the housing.
Analysis 2	The relationship between the heater power and the average temperature of the housing.	Obtain the heater power required for controlling the temperature of the housing at 295.15 K.

Analysis model

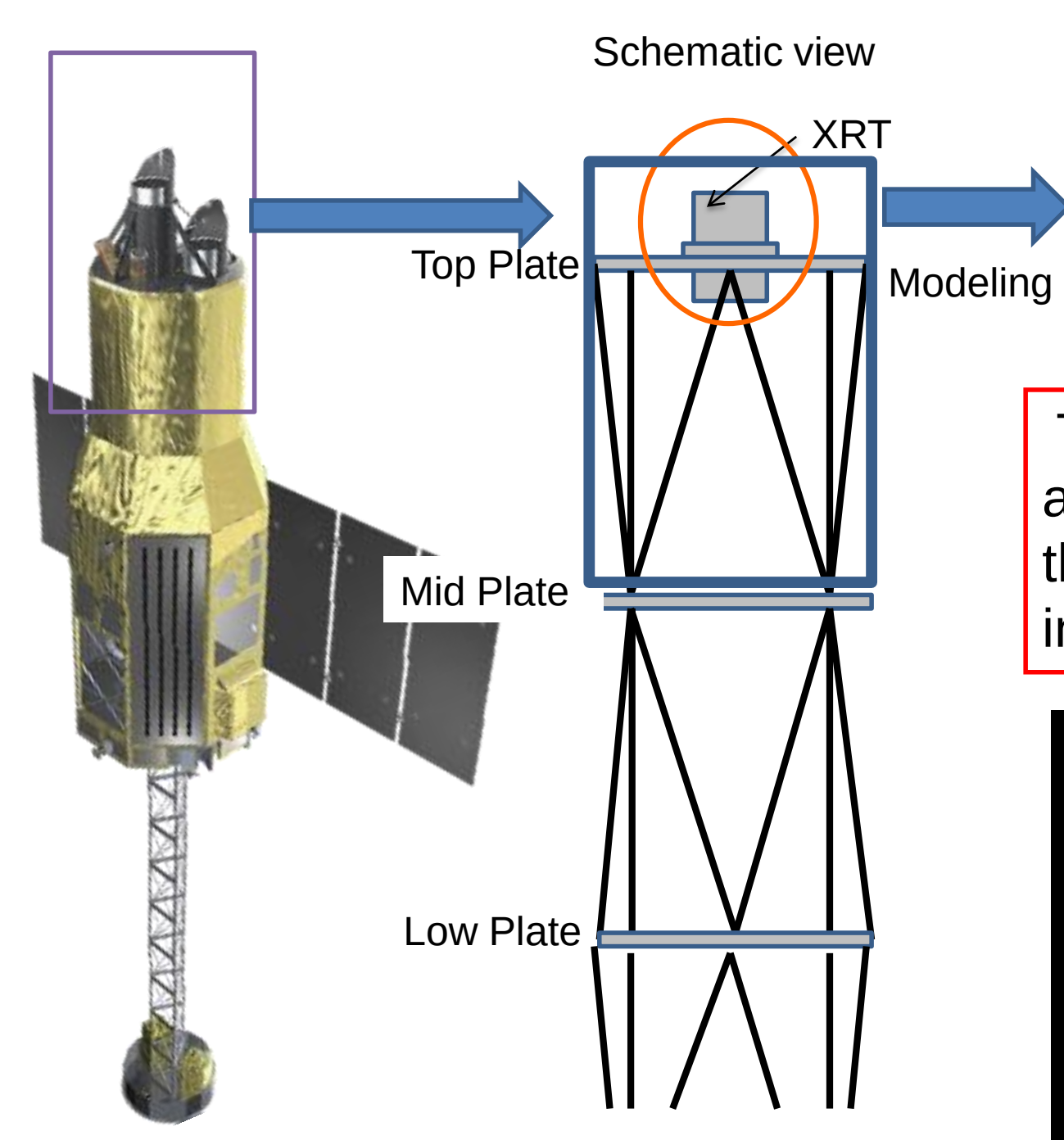

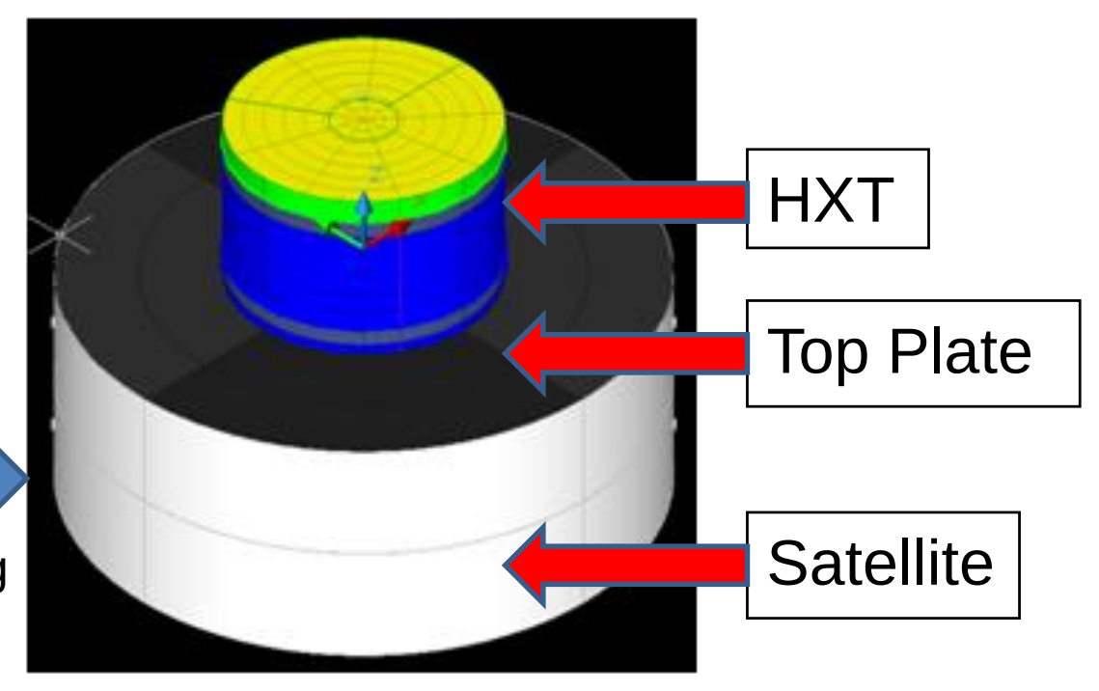

The satellite in the model was simplified and simulated by a cylinder. In addition, the satellite was treated as a blackbody in the radiation analysis.

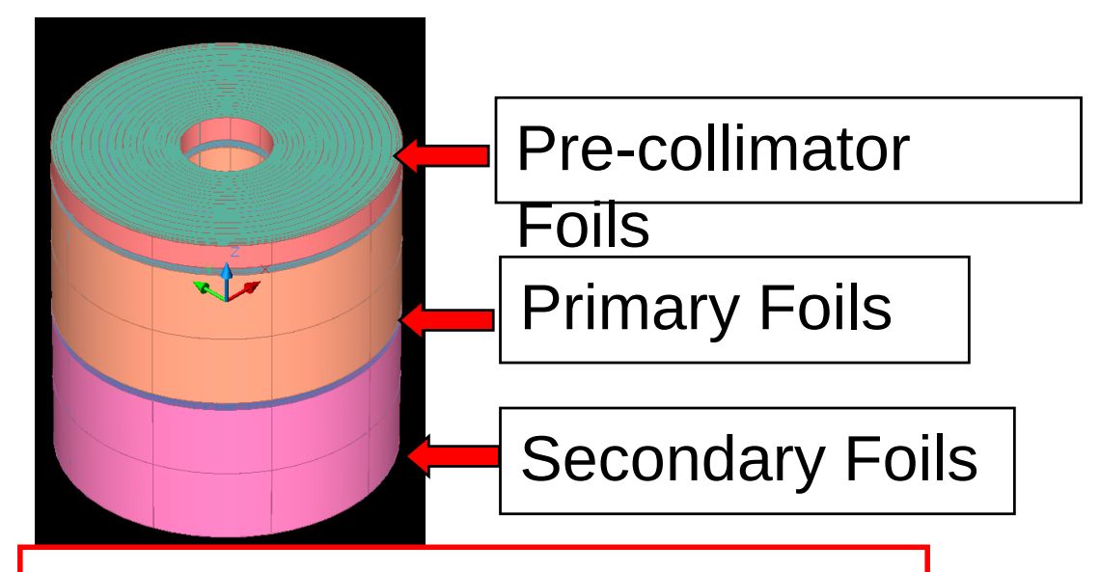

The foils are numbered from the inner to the outer foils.

Thermal properties

	heat conductivity (W/mm/K)	density (kg/mm³)	specific heat (J/kg/K)
A5052	0.138	2.680×10^{-6}	900
A7075	0.121	2.800×10^{-6}	900
MLI	0.001	1.000×10^{-9}	1
Satellite	0.001	1.000×10^{-9}	1
Top Plate	0.05	7.000×10^{-7}	100
Thermal Shield	0.104	2.598×10^{-6}	951.43

Optical properties

	solar absorptivity	infrared emissivity
Foil		
Al	0.263	0.042
Pt	0.401	0.258
Pre-collimator foil	0.23	0.07
Housing		
Aluminum Tape	0.23	0.07
Alumite	0.6	0.6
Thermal Shield		
PET	0.25	0.16
Aluminum	0.23	0.07
Satellite	1	1
Top Plate (CFRP)	0.1	0.05
Top Plate (MLI)	0.32	0.57

The result of analysis 1

Analysis conditions

1. The temperature of the housing was fixed at 295.15 K
2. The temperature of the satellite was set to be 276.05 K and 296.35 K in the analysis for Cold and Hot Cases, respectively.
3. Radiation between the outer surface of the model and the space, a blackbody at 0 K, was considered.

Temperature of the foil #144.

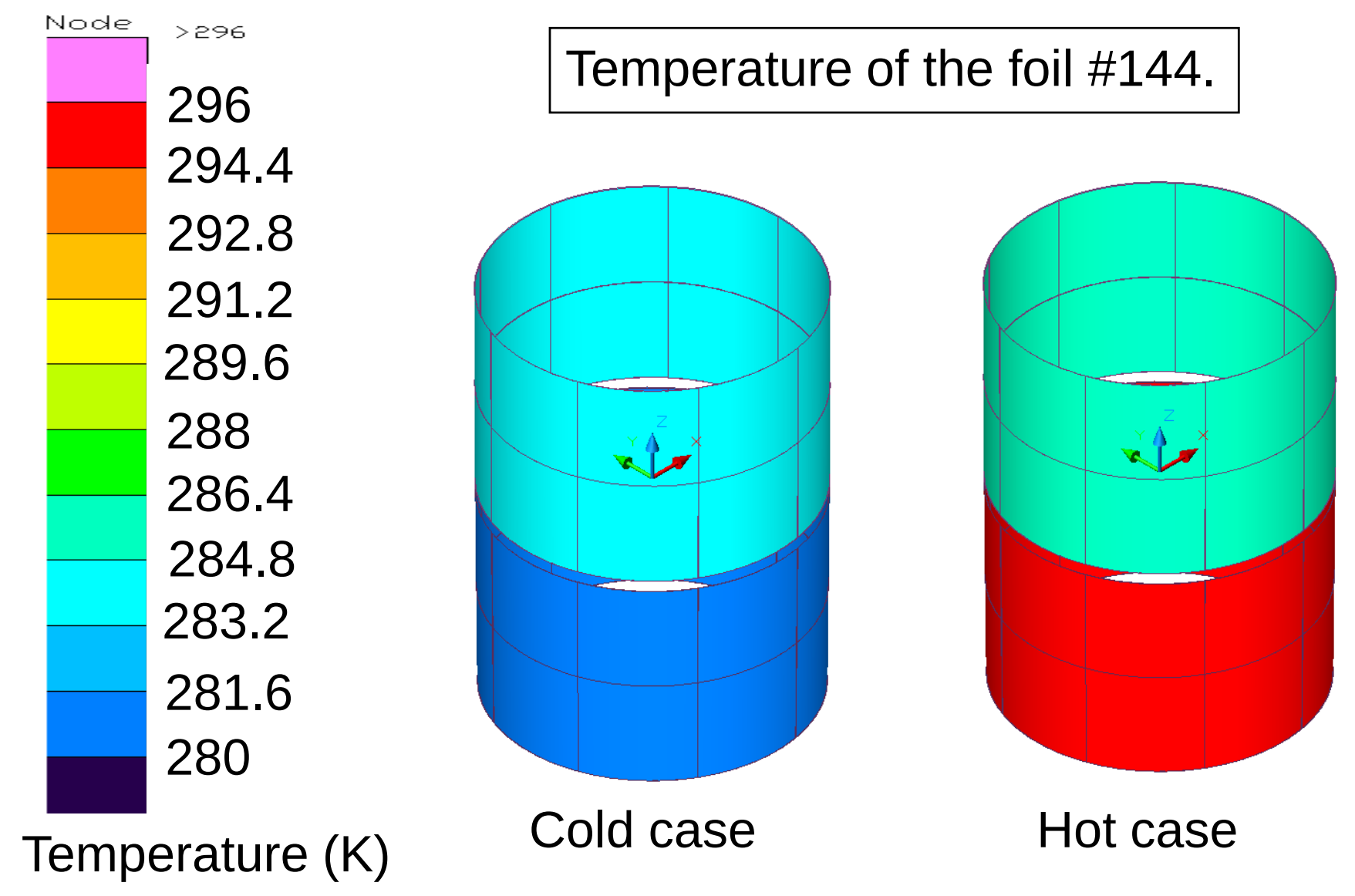

Cold case
Hot case

Temperature gradient hardly appears in one foil.

Temperature of the foils in the radial direction.

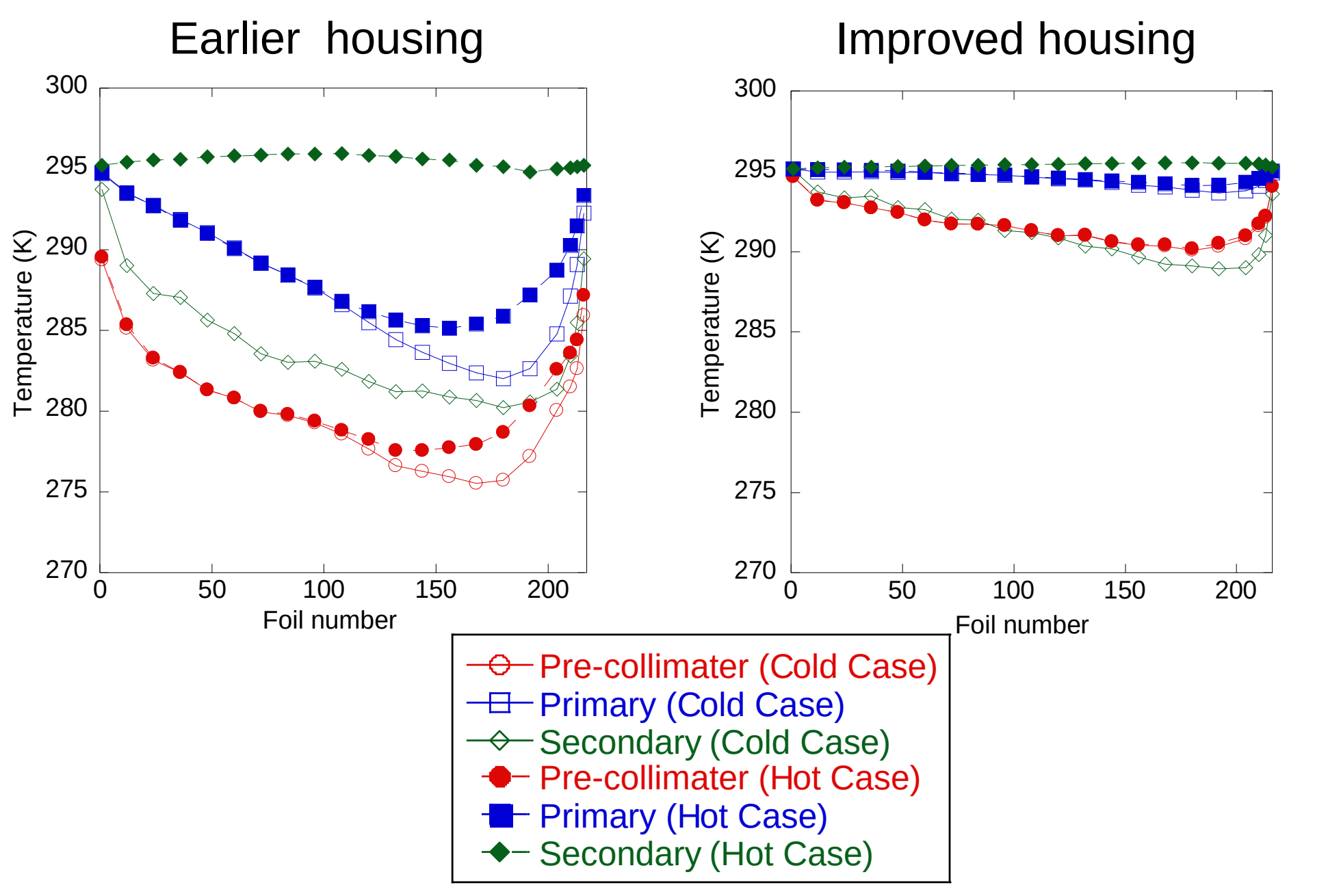

The temperature of the foils in the current design deviates greatly from the target temperature. Therefore, we propose black anodic coating to the inner surfaces of the housing. The temperature of the primary and secondary foils is within the target temperature range in Hot Case. The temperature of the secondary foils for Cold Case is still 4 to 5 K lower than the target temperature.

The result of analysis 2

Analysis conditions

1. Varying the heat applied to the housing from 0 to 20 W in an increment step of 2.5 W. the total heat applied to the housing was equally divided. The divided heat was then applied to the nodes.
2. The temperature of the satellite was fixed at 276.05 K.
3. Radiation between the outer surface of the model and the space, a blackbody at 0 K, was considered.

The average temperature of the housing becomes 295.15 K when of 17 W is given to the housing.
The housing is uniformly heated.

Relationship between heater power and average temperature of the housing.

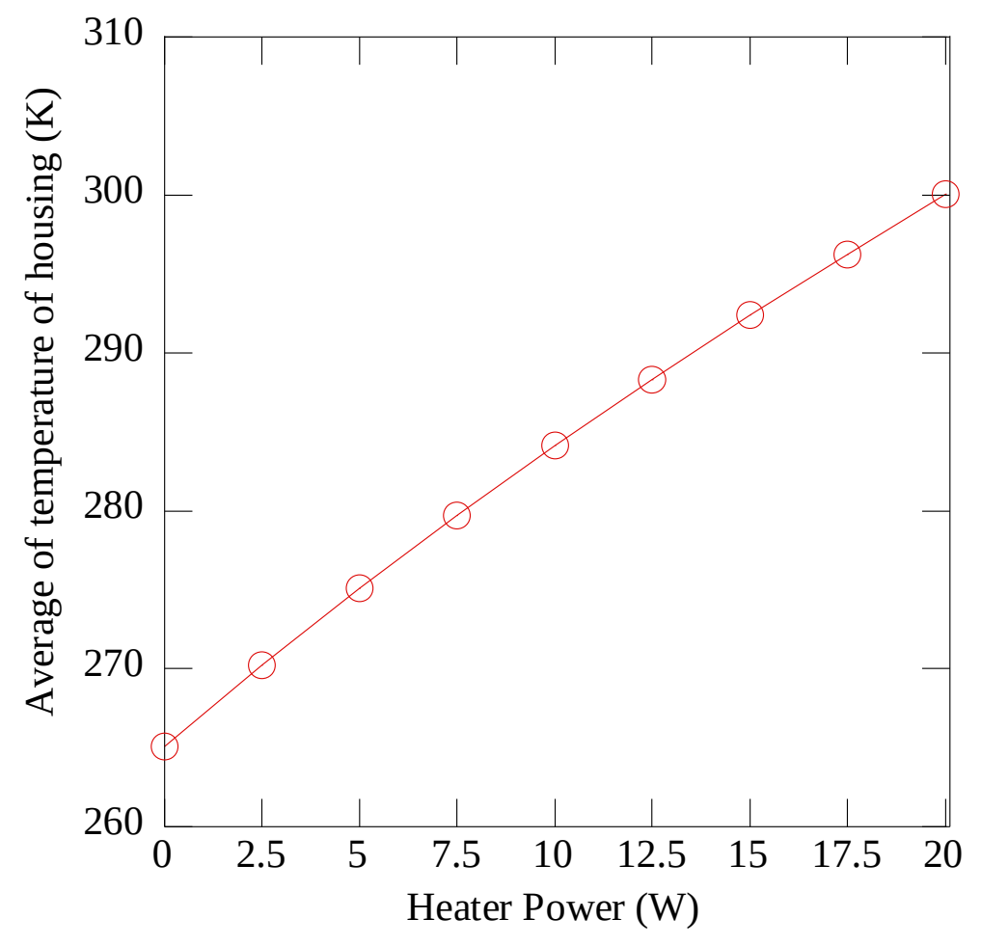

Temperature distribution for the heater power of 17 W.

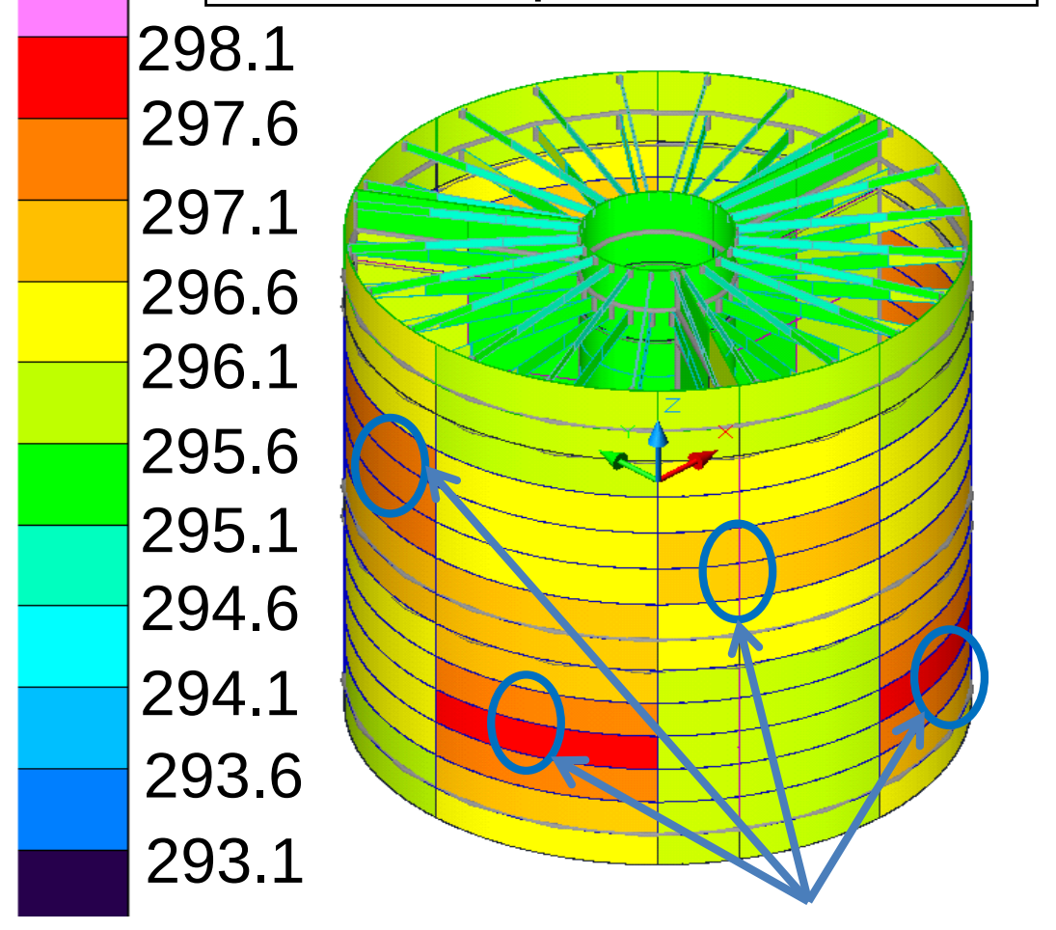

The investigation of the deformation of the mirror foil due to temperature change

Outline

We analyzed the following three cases in order to quantitatively evaluate thermal deformation of the foil.
Case 1: free thermal expansion without constraint of deformation.
Case 2: thermal expansion with the periodical constraint by the alignment bars.
Case 3: both edges of the foil are constrained by the alignment bars.
The real constraint condition is expressed by Case 3.

For Case I, two-dimensional (2D) and three-dimensional (3D) finite element analysis (FEA) was performed while the curved laminate beam theory was employed for prediction of thermal deformation.
For Case 2, 2D and 3D FEA in addition to prediction using the beam theory was conducted.
For Case 3, only 3D FEA was performed.

FEA

Quasi-static thermal deformation analysis was performed using a commercial FE software (Abaqus, Simulia). The 2D model without constraint at the left edge corresponds to Case 1. In contrast, the 3D model, where the deformation in the *x*- and *z*-directions is constrained on the symmetry planes (curves BD and CD), corresponds to Case 1. When the symmetry boundary condition at the curve AC is added to the above boundary conditions, the model corresponds to Case 3. Then, the curve BD represents the central generating line between the alignment bars.

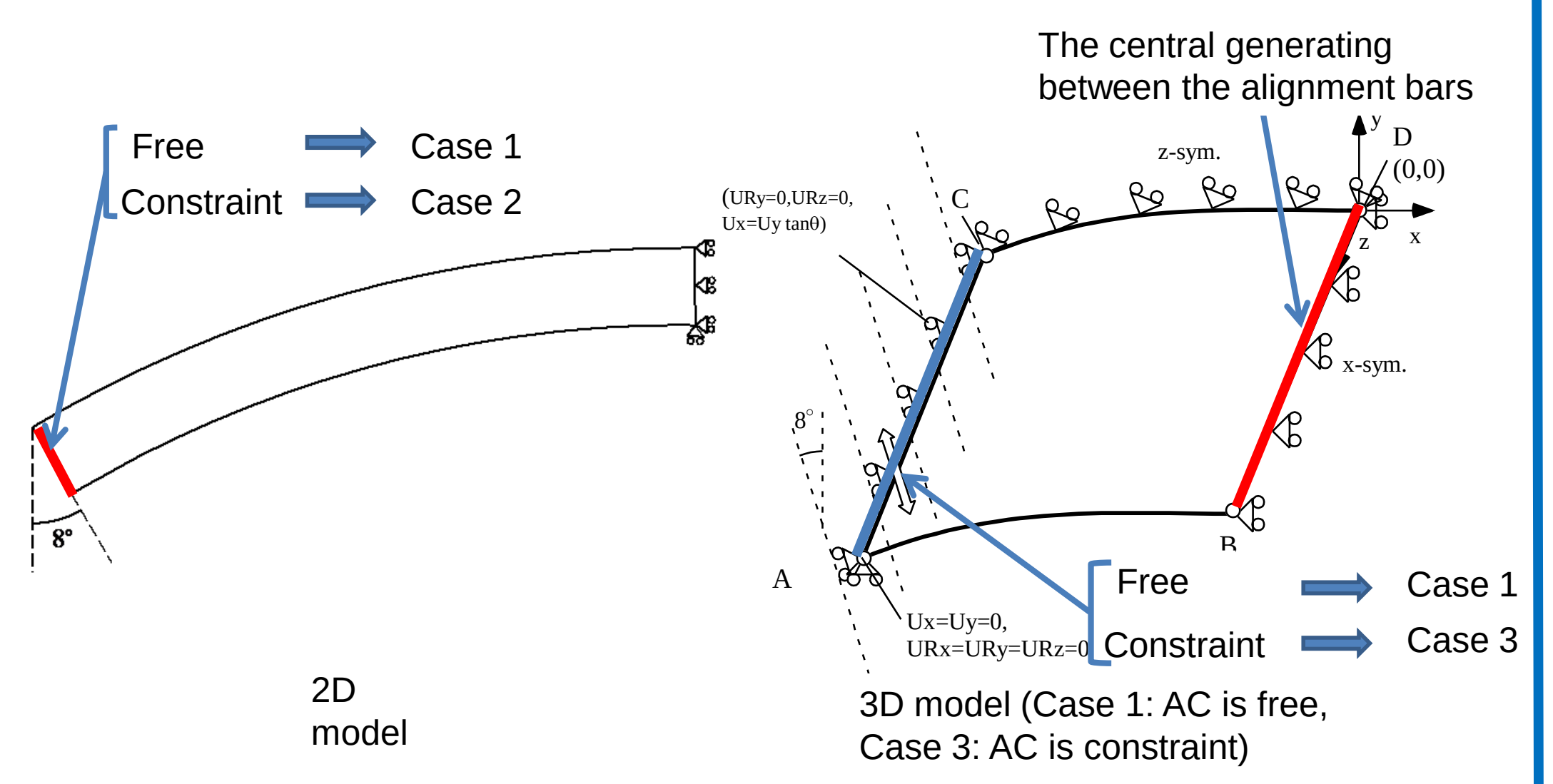

2D model

3D model (Case 1: AC is free, Case 3: AC is constraint)

Thickness and material properties of constituent layers

layer	thickness (μm)	young's modulus (GPa)	poisson ratio	linear coefficient of expansion 10^{-6} K^{-1}
reflection coating	0.1	168	0.377	8.8
epoxy	20	3.1	0.34	50
aluminum	200	70	0.34	23

Curved laminate beam theory

Case1

Let the foil be regarded as a curved laminate beam, that consists of *n* layers and has the initial curvature of ρ_0.

The longitudinal strain

$$\varepsilon_0=\frac{(\rho_0\beta+\gamma)\nu+\beta\mu}{(\alpha+\beta)\gamma+\rho_0\alpha\beta}\Delta T$$

$$\alpha=\sum_{k=1}^{n}E_kt_k,\ \beta=\sum_{k=1}^{n}E_kt_k\kappa_k,\ \gamma=\sum_{k=1}^{n}E_k\frac{{y_k}^2-{y_{k-1}}^2}{2}$$

The angular strain

$$\omega=\frac{\rho_0\beta\nu+(\alpha+\beta)\mu}{(\alpha+\beta)\gamma+\rho_0\alpha\beta}\Delta T$$

$$\mu=\sum_{k=1}^{n}E_k\frac{{y_k}^2-{y_{k-1}}^2}{2}\alpha_k,\ \nu=\sum_{k=1}^{n}E_kt_k\alpha_k$$

The curvature change due to temperature change

$$\frac{1}{\rho}-\frac{1}{\rho_0}=\frac{1}{\rho_0}\frac{\alpha\mu-\gamma\nu}{(\alpha+\beta)\gamma+\rho_0\alpha\beta}\Delta T$$

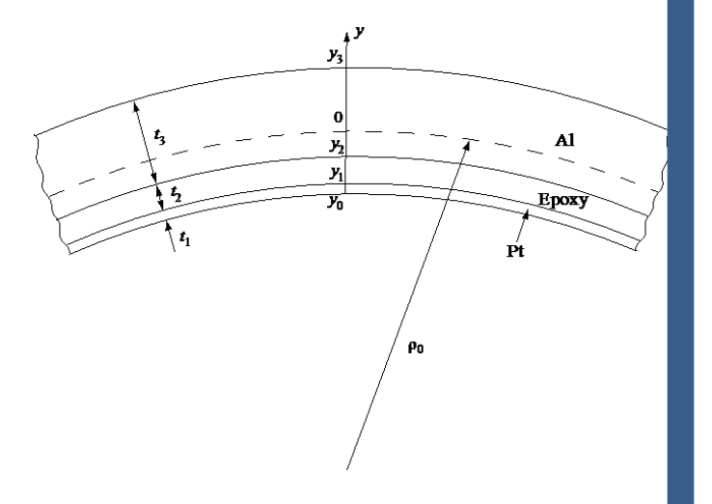

Case1

Case2

The central angle of the arcs divided by the alignment bars is 16 degrees. The displacement in the *y*-direction at the center of the arc is computed as

$$v\big|_{\varphi=\theta}=\frac{\rho_0}{C_1A}\left(-C_3\beta+2C_2(\alpha+\beta)\right)(\gamma+\alpha\rho_0)\theta(1-\cos\theta)(1-\sin\theta)\Delta T$$

E_k denotes the Young‘s modulus, α_k the coefficient of thermal expansion, t_k the thickness, and K_k the coefficient of area of the *k*-th layer. In addition, *μ* and *v* represent the axial moment and force per width and per temperature change, ΔT the temperature change, and y_k and y_k*-1* the *y*-coordinates at the top and bottom of the *k*-th layer.

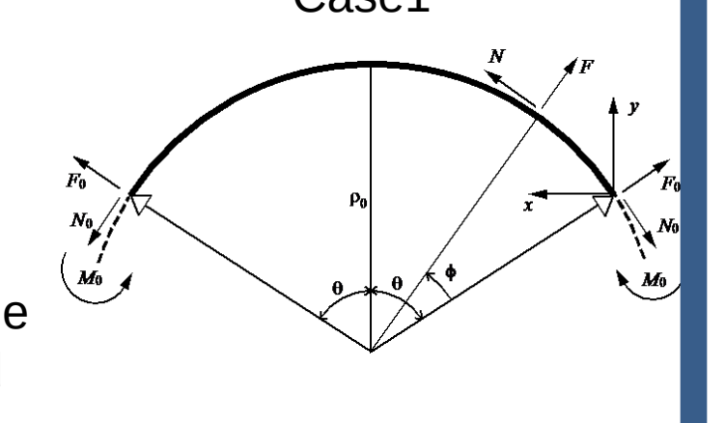

Case2

Measurement of thermal deformation

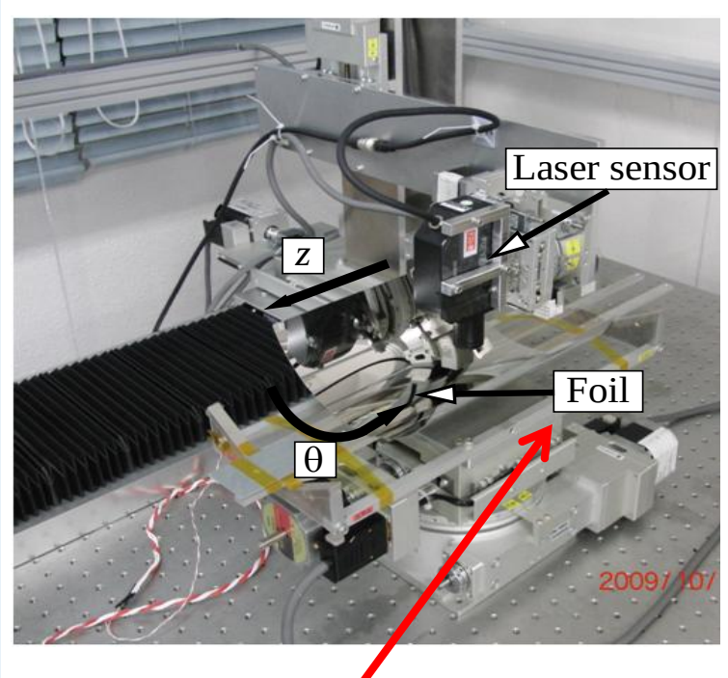

A foil with the initial radius of 100 mm and the generating line length of 200 mm.

The temperature of the foil was controlled by cooling or heating the air in the booth using the heater and the air conditioner. The 3D geometry of the foil at 22, 26 and 30 ºC was measured, rotating the laser sensor in the hoop (θ) direction from -55 to +55 degrees, as well as traversing the sensor in the *z*-direction.

The data taken from the experiment was transformed to the change in radius of curvature using following equation.

$$\Delta=(\rho_0-\rho_1)\left\{1-\cos\varphi-\frac{1}{2}\left(1-\frac{r^2}{\rho_0\rho_1}\right)\sin^2\varphi\right\}$$

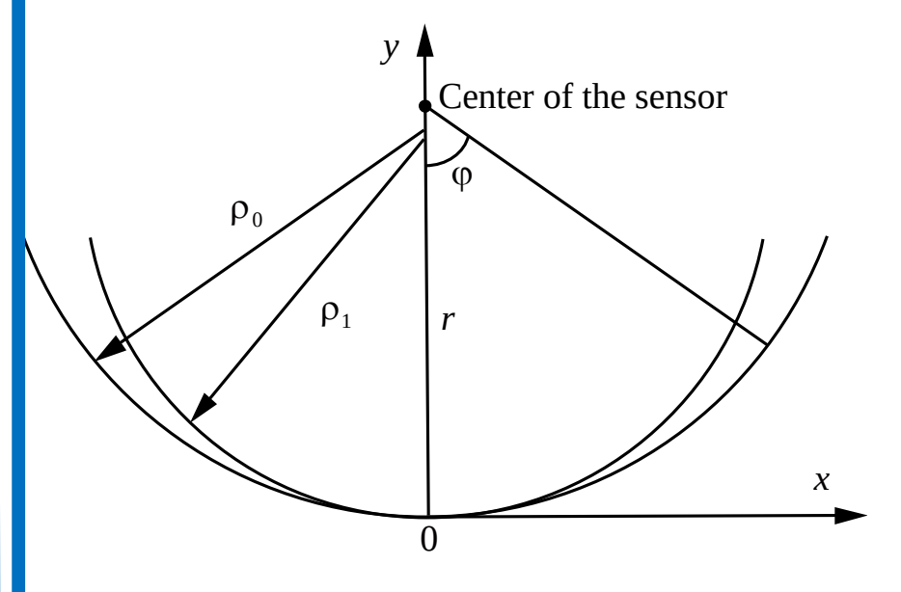

Specific of laser sensor (LT-9030M)

measurement range	±1mm
basis distance	30mm
scan range/scan step	0～560μm/1～8μm
resolution	0.1μm
linearity	±0.3% of F.S.
sampling period	670μs～187ms

Result (All the following results are the calculations for the temperature change of 1 degree.)

Case1

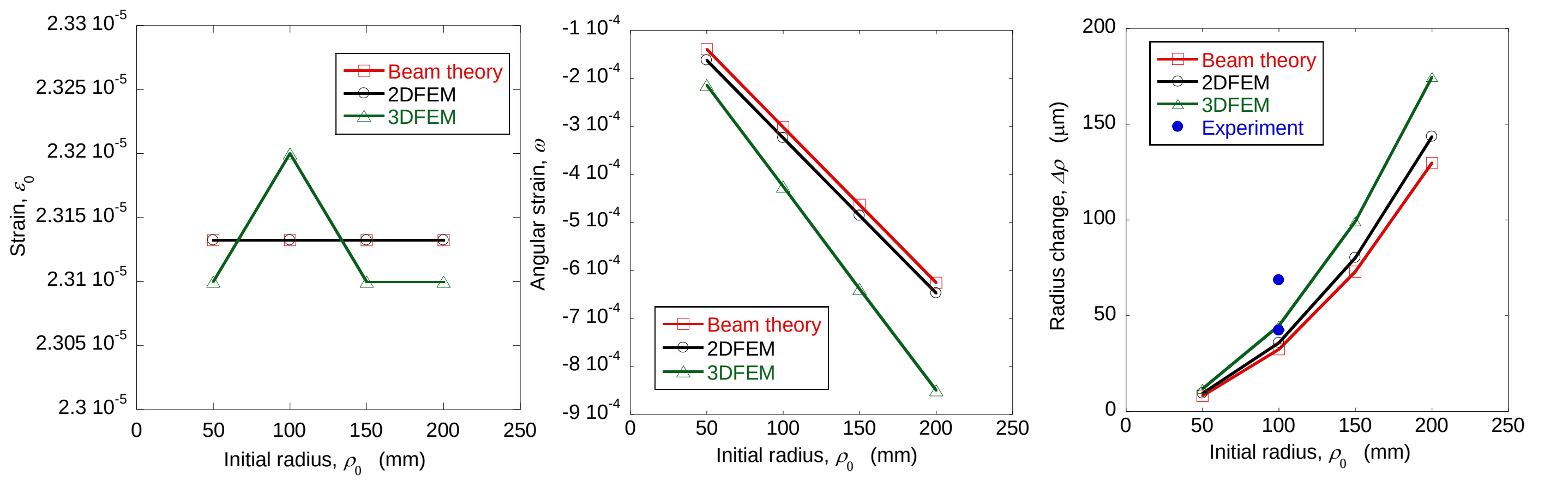

Axial strain
Angular strain
Change in radius of curvature

The change in the is larger in the ⊿ρ outer foils, for example, ⊿ρ=140～180 mm for ⊿ρ=200 mm. The theoretical values of ω and ⊿ρ are in good agreement with the results of 2D FEA, while the results of 3D FEA are 20 to 30 % larger than them.

Case2

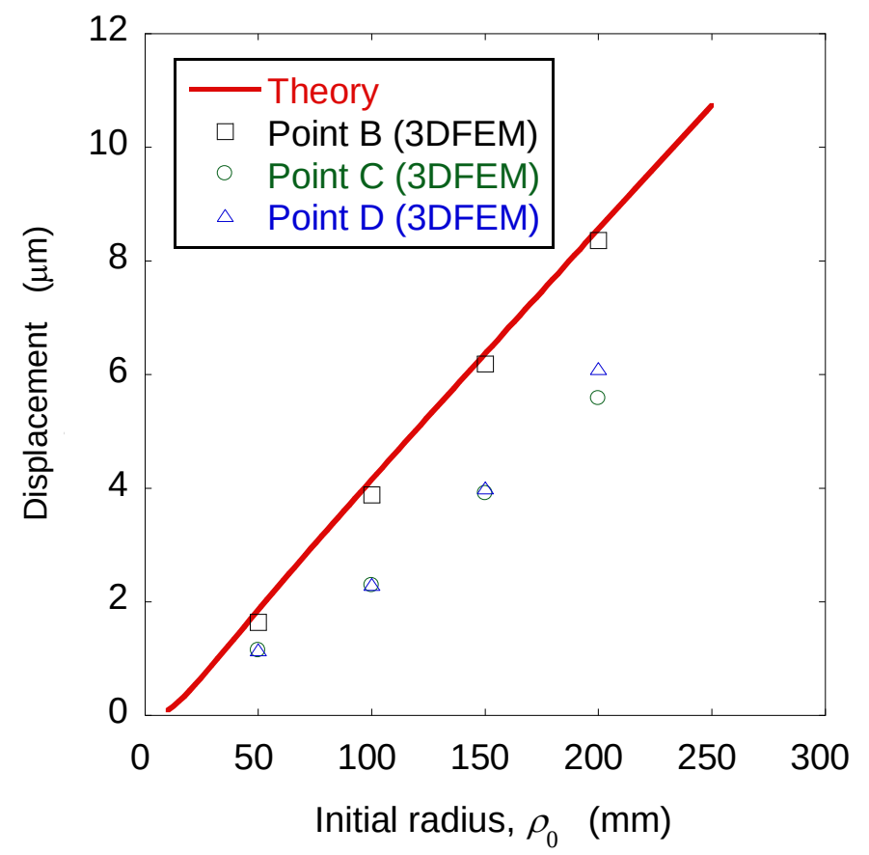

The theoretical displacement at the center for Case 2 (Eq. (5)), in addition to the displacements at the points B, C and D in the 3D FEA for Case 3.

The theoretical displacement agrees well with that at the point B.

The displacements at the points C and D are smaller than that at the point B. Thus, the beam theory for Case 2 cannot predict the displacement accurately.

Case3

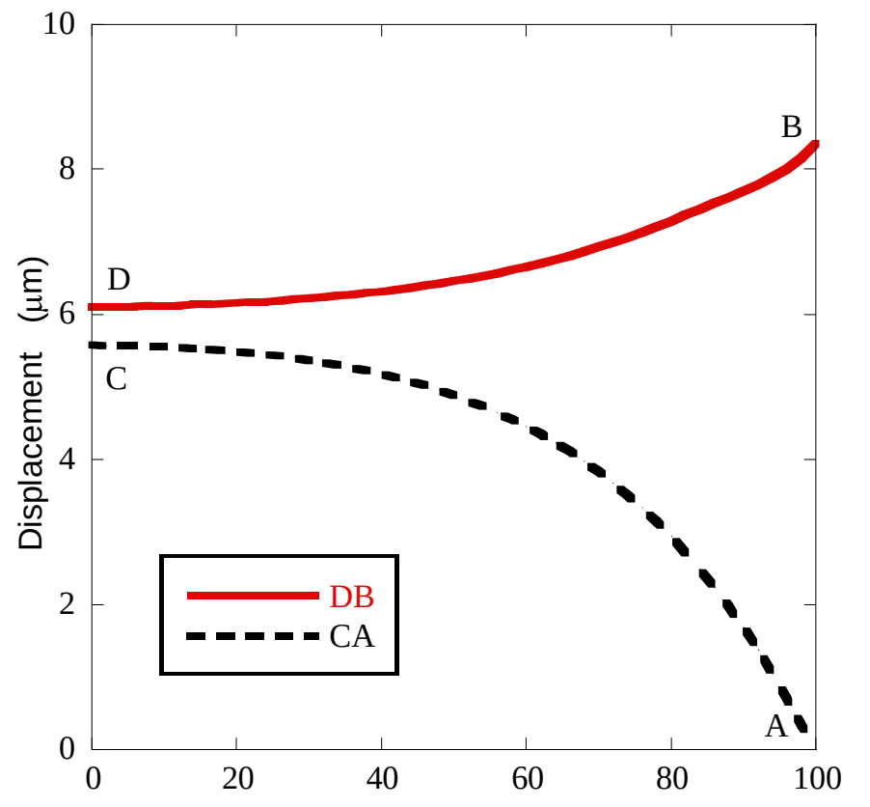

Displacement along the generating line (Case 3, ρ_0 =200mm)

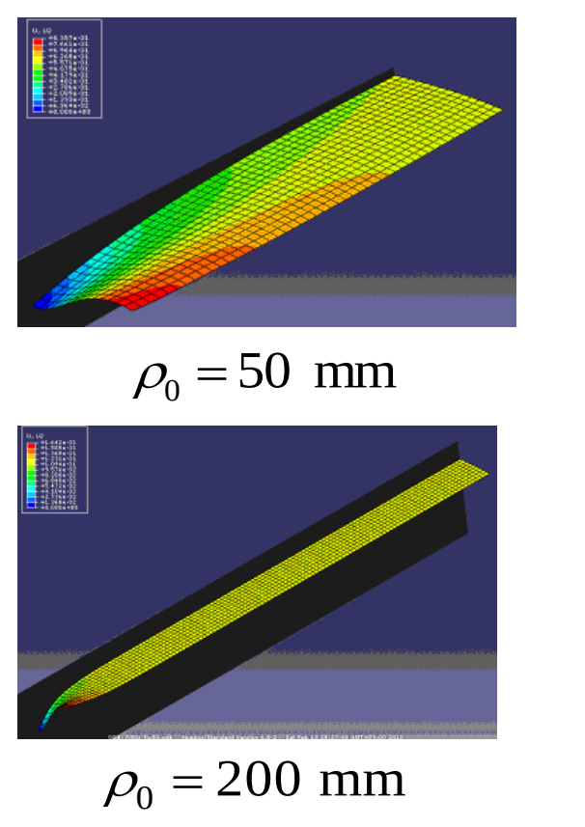

Deformation for Case 3

The foil is twisted due to thermal deformation. The deformation is limited near the edge (curve AB) in the foil with small ρ_0, while the foil with larger ρ_0 is deformed along the length direction. For ρ_0=200mm, the deformation is 5.6 μm along the generating line AC, which passes through the supporting points of the alignment bars.

Conclusion

1. The temperature of the foils is kept at the target temperature by anodizing the housing.
2. The temperature of the secondary foils depends largely on the temperature in the satellite. Hence, it is necessary to control the temperature in the satellite, or to equip the thermal shield at the bottom of the housing.
3. Temperature change must be limited to below 1.8 K for controlling the deformation of the foil along the generating line to less than 10 μm.

REFERENCES
[1] Ko, W. L. and Jackson, R. H. , Mutilayer theory for delamination analysis of a composite curved bar subjected to end forces and end moments, NASA TM 4139 (1989).
[2] Kress, G., Roos, R., Barbezat, M., Dransfeld, C. and Ermanni, P., Model for interlaminar normal stress single curved laminates, Composite Structures, 69 (2005), pp.458-469.
[3] Lin, K. C. and Hsieh, C. M., The closed form general solutions of 2-D curved laminated beams of variable curvatures, Composite Structures, 79 (2007), pp.606-618..
[4] Endo, S., Thermoelastic Equations for Multi-Layered Cylindrical Shells, Technical Report of National Aerospace Laboratory TR-1222 (1994).
[5] Naidu, N. V. S. and Sinha, P. K., Nonlinear finite element analysis of laminated composite shells in hgyrothermal environment, Composite Structures, 69(2005), pp.387-395.
[6] Futamura, M., Miyake, T., Fujiyoshi, T., Fukuzawa, S., Ohno, N., Residual Stresses Depending on Changes of Temperature and Water Absorption in Carbon Fiber/Epoxy Single-Fiber Model Composites, Material, Vol. 57（2008）, No. 5, pp.442-447.
[7] Ogasaka, Y., Tamura, k., Miyazawa, T., Fukaya, Y., Iwahara, T., Sasaki, N., Furuzawa, A., Haba, Y., Kanou, Y., Ueno, D., Kunieda, H., Yamashita, K., Shibata, R., Okajima, T., Tueller, J., Serlemitsos, P., Soong, Y., Chan, K.-W., Miyata, E., Tsunemi, H., Uesugi, K., Suzuki, Y., and Namba, Y., Thin-foil multilayer-supermirror hard x-ray telescopes for InFOCμS/SUMIT balloon experiments and NeXT satellite program, Optics for EUV, X-Ray, and Gamma-Ray Astronomy III. Edited by O'Dell, Stephen L.; Pareschi, Giovanni. Proceedings of the SPIE, Vol. 6688, pp. 668803 (2007).
theory were verified. This verification enables us to predict the thermal deformation for Case 3, whose measurement is difficult.